Letter

Unexpectedly enhanced α-particle preformation in ^{48}Ti probed by the $(p, p\alpha)$ reaction

Yasutaka Taniguchi,[1,2,*] Kazuki Yoshida,[3,2] Yohei Chiba,[4,5,2] Yoshiko Kanada-En'yo,[6,2] Masaaki Kimura,[7,8,2] and Kazuyuki Ogata[2,4,5]

[1]*Department of Information Engineering, National Institute of Technology (KOSEN), Kagawa College, Mitoyo, Kagawa 769-1192, Japan*
[2]*Research Center for Nuclear Physics (RCNP), Osaka University, Ibaraki 567-0047, Japan*
[3]*Advanced Science Research Center, Japan Atomic Energy Agency, Tokai, Ibaraki 319-1195, Japan*
[4]*Department of Physics, Osaka City University, Osaka 558-8585, Japan*
[5]*Nambu Yoichiro Institute of Theoretical and Experimental Physics (NITEP), Osaka City University, Osaka 558-8585, Japan*
[6]*Department of Physics, Kyoto University, Kyoto 606-8502, Japan*
[7]*Department of Physics, Hokkaido University, Sapporo 060-0810, Japan*
[8]*Nuclear Reaction Data Centre, Hokkaido University, Sapporo 060-0810, Japan*

(Received 7 December 2020; accepted 16 March 2021; published 24 March 2021)

The formation of α particles on nuclear surfaces has remained a fundamental problem since the dawn of nuclear physics. This α-particle formation strongly affects the α-decay lifetimes of heavy and superheavy elements, level scheme of light nuclei, and synthesis of elements in stars. However, despite its importance, the α-particle formation in medium-mass nuclei is seldom investigated. Based on the ^{48}Ti$(p, p\alpha)^{44}$Ca reaction analysis, this study reports that α-particle formation in the medium-mass ^{48}Ti nucleus is pronounced more compared to that expected through mean-field approximations. Moreover, the estimated average distance between the α particle and residue equals approximately 4.5 fm. This result poses a challenge to describe the four nucleon correlations using microscopic nuclear models.

DOI: 10.1103/PhysRevC.103.L031305

Introduction. Since Gamow [1] explained α decay as the quantum tunneling of α particles out of the atomic nucleus, the formation of α particles on nuclear surfaces has attracted significant research attention to understand the structure and decay of atomic nuclei [2–5]. This formation of α particles usually occurs on low-density nuclear surfaces that possess a certain probability to this end. This probability is referred to as the preformation factor or α-particle-preformation probability and determines the lifetimes of heavy and superheavy nuclei. This probability is usually evaluated considering the α-decay lifetimes of elements. For instance, using this approach, recent studies have evaluated the very short lifetimes of ^{108}Xe and ^{104}Te [6,7], as well as realized enhancement in the α-particle-preformation probability beyond that of the proton-rich ^{100}Sn nucleus [8–11].

Furthermore, α-particle preformation manifests as α clustering [12,13] in light nuclei. This phenomenon is closely related to the synthesis of elements in stars [14,15]. Owing to its unique excitation spectra, α clustering has been realized in several light nuclei [16,17]. However, compared to the above-mentioned heavy- and light-mass nuclei, the realization of α-particle preformation in medium-mass nuclei is seldom investigated. Generally, it is reckoned that α-particle preformation is inhibited in medium-mass nuclei owing to the largely negative α-decay Q-values. The large binding energies in these nuclei also lead to the dominance of mean-field dynamics over the four nucleon correlations, thereby inhibiting α-particle formation. However, such inhibitions have never been quantitatively confirmed via experiments owing to the lack of a reliable measure for α-particle preformation.

The proton-induced α-knockout reaction $(p, p\alpha)$ has been considered a sensitive means to confirm α-particle preformation [18–22]. Owing to their strong absorption effect, the α particle kicked by the projectile proton cannot be removed from the target-nucleus interior. Consequently, the reaction is only sensitive to the formation of α particles on the target-nucleus surface. Several experiments have been conducted to measure the α-particle-preformation probability in the light- and medium-mass nuclei. Carey *et al.* proposed a means to perform systematic measurements during $(p, p\alpha)$ reactions involving different target nuclei from ^{16}O to ^{66}Zn [20]. However, mainly because of the use of a phenomenological α wave function without internucleon antisymmetrization, the absolute value of the α-particle-preformation probability deduced from the cross sections demonstrated a significant uncertainty.

Recently, the use of the distorted wave impulse approximation (DWIA) framework with reliable optical potentials has been reported to provide an accurate description of the $(p, p\alpha)$ reaction [23]. For example, their study quantitatively evaluated the α-particle-preformation probability of the light-mass α-clustered ^{20}Ne nucleus. The corresponding results revealed that the α-particle-preformation probability of ^{20}Ne is half of that estimated by Carey *et al.* Among the nuclei studied by Carey *et al.*, ^{48}Ti and ^{20}Ne were the only ones for which the

*taniguchi-y@di.kagawa-nct.ac.jp

optical potentials between a proton, α particle, residue (^{44}Ca), and target nucleus were accurately known [24–26]. Furthermore, the residue ^{44}Ca represents a stable magic nucleus with an inert core. Therefore enhancement of the α-particle-preformation of the target nucleus can be expected. Thus the DWIA analysis of the ^{48}Ti$(p, p\alpha)^{44}$Ca reaction is expected to shed new insight pertaining to α-particle preformation in medium-mass nuclei.

DWIA framework. In this study the DWIA framework [23,27–29] was adopted to describe the ^{48}Ti$(p, p\alpha)^{44}$Ca reaction. Within the factorization approximation, the triple-differential cross section could be expressed as

$$\frac{d^3\sigma}{dT_p d\Omega_p d\Omega_\alpha} = C_0 F_{\rm kin} \frac{d\sigma_{p\alpha}}{d\Omega_{p\alpha}} |\bar{T}|^2, \tag{1}$$

where T_p, Ω_p, and Ω_α denote the kinetic energy of the emitted proton and solid angles of the said proton and α particles, respectively. Further, $C_0 F_{\rm kin}$ denotes the kinematical factor, and $d\sigma_{p\alpha}/d\Omega_{p\alpha}$ denote the p-α-differential cross section corresponding to the p-α relative momentum of the $(p, p\alpha)$ reaction kinematics. The details concerning this approximation and the corresponding validation could be found in Refs. [27,28]. The reduced transition-matrix element $\bar{T}$ could be expressed as

$$\bar{T} = \int d^3R\, F(\boldsymbol{R}) y(R) Y_{00}(\hat{\boldsymbol{R}}), \tag{2}$$

$$F(\boldsymbol{R}) = \chi_p^{*(-)}(\boldsymbol{R}) \chi_\alpha^{*(-)}(\boldsymbol{R}) \chi_p^{(+)}(\boldsymbol{R}) e^{-i\boldsymbol{k}_0 \cdot \boldsymbol{R}/12}, \tag{3}$$

where $\boldsymbol{k}_0$ denotes the incident-proton momentum. Equation (2) facilitates the evaluation of the sensitivity of the cross section to α-particle preformation because it depends on the probability amplitude of the α-particle preformation $y(R)$. The other analysis components represent the optical potentials for p-^{48}Ti, p-^{44}Ca, and α-^{44}Ca scattering, which are used to describe the distorted waves—$\chi_p^{(\pm)}(\boldsymbol{R})$ and $\chi_\alpha^{(-)}(\boldsymbol{R})$. The superscripts $(+)$ and $(-)$ indicate the outgoing and incoming boundary conditions, respectively. The use of accurate optical potentials is demonstrated to be essential to obtain a precise description and evaluation of the cross sections and α-particle preformation, respectively. In this study we applied the EDAD1 optical potential [25,26,30] with Dirac phenomenology to the p-^{48}Ti and p-^{44}Ca distorted waves. This facilitated the realization of the elastic proton-nucleus scattering with various stable targets (from ^{12}C to ^{208}Pb) over a wide energy range (between 20 MeV and 1 GeV). For the α-^{44}Ca distorted wave, we applied the optical potential proposed by Delbar *et al.* [24], which accurately reproduces the elastic differential cross sections between 24.1 and 100 MeV. These potentials cover the required energy range for analyzing the ^{48}Ti$(p, p\alpha)^{44}$Ca reaction.

α-particle preformation probability. The amplitude of the α-particle preformation probability is called the reduced-width amplitude (RWA), expressed as

$$y(R) = \sqrt{\frac{48!}{4!\,44!}} \langle \delta(r - R) \Phi_\alpha \Phi_{\rm Ca} Y_{00}(\hat{r}) | \Phi_{\rm Ti} \rangle / R^2, \tag{4}$$

where Φ_α, $\Phi_{\rm Ca}$, and $\Phi_{\rm Ti}$ denote the ground-state wave functions of the α particle, residue (^{44}Ca), and target nucleus (^{48}Ti), respectively. In this study, α was assumed to possess a $(0s)^4$ configuration; further, the ^{44}Ca and ^{48}Ti wave functions were described using the antisymmetrized molecular dynamics (AMD) [31–33]. The parity-projected AMD wave function can be expressed as

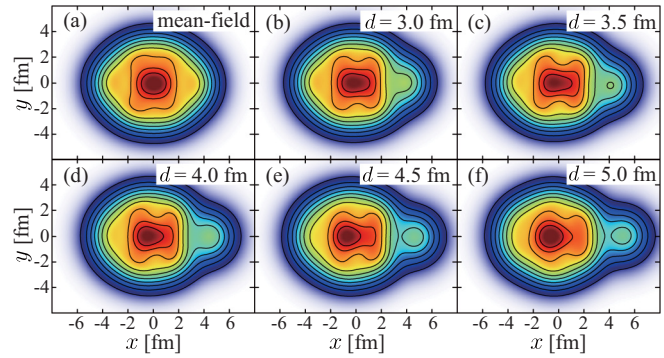

FIG. 1. Wave-function density distributions for RWA calculation—(a) mean-field solution; (b)–(f) $\alpha + ^{44}$Ca system with different internuclear distances d.

$$\Psi = (1 + P_x)/2 \times \mathcal{A}\{\, \varphi_1 \varphi_2 \ldots \varphi_A \,\}, \tag{5}$$

$$\varphi_i = \prod_{\sigma=x,y,z} \exp\{\, -\nu_\sigma (r_\sigma - Z_{i\sigma})^2 \,\} \times (\alpha_i |\uparrow\rangle + \beta_i |\downarrow\rangle) \times (|p\rangle \text{ or } |n\rangle), \tag{6}$$

where P_x denotes the parity operator, $\mathcal{A}$ denotes the antisymmetrizer, and φ_i denotes the nucleon wave packet. The centroid of the nucleon wave packet comprises a complex vector $\boldsymbol{Z}_i$, the real and imaginary parts of which describe the mean position and momentum of a nucleon, respectively. The model wave-function parameters include the centroid ($\boldsymbol{Z}_i$), spin directions (α_i and β_i) and Gaussian widths (ν_x, ν_y, and ν_z). The ^{44}Ca wave function was calculated within the mean-field approximation, i.e., the parameters are optimized to minimize the intrinsic energy $E = \langle \Psi | H | \Psi \rangle / \langle \Psi | \Psi \rangle$. Here, the Hamiltonian comprises the nucleon kinetic energies, Coulomb interaction, and effective nucleon-nucleon interaction. The Gogny D1S density functional [34], which reasonably reproduces the fundamental nuclear properties, was considered the above-mentioned nucleon-nucleon interaction in this study. After energy minimization, the ^{44}Ca wave function was projected onto $J^\pi = 0^+$ to calculate RWA [Eq. (4)] using the Laplace expansion method [35].

The ^{48}Ti wave function was similarly calculated. This wave function, i.e., the mean-field solution for ^{48}Ti, is shown in Fig. 1(a). It demonstrates a near-spherical shape without α-particle preformation. Indeed, the RWA calculated using this mean-field solution [Fig. 2(a)] demonstrates a small peak at $R = 4.8$ fm. This peak, as discussed later, is too small to reproduce the observed cross section. Therefore we artificially generated the ^{48}Ti test wave function that exhibits prominent α-particle preformation. Accordingly, an approximate internuclear distance d [36,37] was introduced; it can be

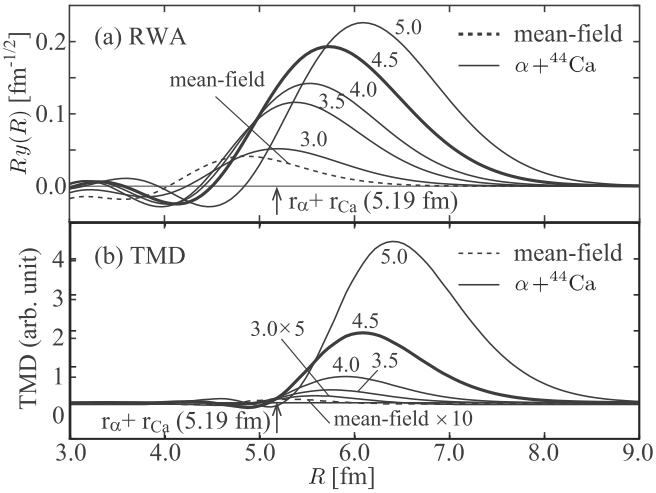

FIG. 2. (a) RWA values calculated from $\alpha + {}^{44}$Ca (d = 3.0–5.0 fm) and mean-field wave functions shown in Fig. 1; (b) TMD values of ^{48}Ti(p, $p\alpha$)^{44}Ca reaction at $T_p = 63$ MeV. The TMD values were calculated using the mean-field solution, and the $d = 3.0$ fm wave function was multiplied by 10 and 5, respectively. The arrow indicates the sum of α and ^{44}Ca charge radii, which approximately correspond to the nuclear surface.

expressed as

$$d = \left| \frac{1}{4} \sum_{i=1,\ldots,4} \mathrm{Re}\boldsymbol{Z}_i - \frac{1}{44} \sum_{i=5,\ldots,48} \mathrm{Re}\boldsymbol{Z}_j \right|, \tag{7}$$

where the first and second terms correspond to the α and ^{44}Ca mass centers, respectively. The energy variations were effected with a constraint on the d value, and wave functions that mimic the α-particle preformation were obtained using different internuclear distances, as shown in Figs. 1(b)–1(f). The distortion of α and ^{44}Ca due to the internucleon antisymmetrization is naturally taken into account because of the microscopic treatment of the AMD. The RWA values calculated using the wave functions shown in Fig. 2(a) demonstrate prominent peaks with gradually increasing maximum values. Further, these peaks move outward with an increase in d. RWAs remain strongly suppressed in the interior of the residual nucleus ($R \lesssim 5$ fm), in accordance with the Pauli principle. Consequently, the peak position need not correspond to the value of d.

Results and discussion. Figure 3 shows the triple-differential cross sections pertaining to the ^{48}Ti(p, $p\alpha$)^{44}Ca reaction obtained via DWIA calculations using the RWAs shown in Fig. 2(a). These cross sections are plotted as functions of the outgoing proton energy. The incident-proton energy and values of the proton and α-particle emission angles were set to those reported by Carey *et al.* [20]. Unexpectedly, the mean-field solution did not reproduce the observed cross section at all. Further, the cross section was underestimated by three orders of magnitude. This cannot be explained based on the uncertainty of the optical potentials used during DWIA analysis or density functional (Gogny D1S) used to calculate the mean-field solution. Therefore the α-preformation

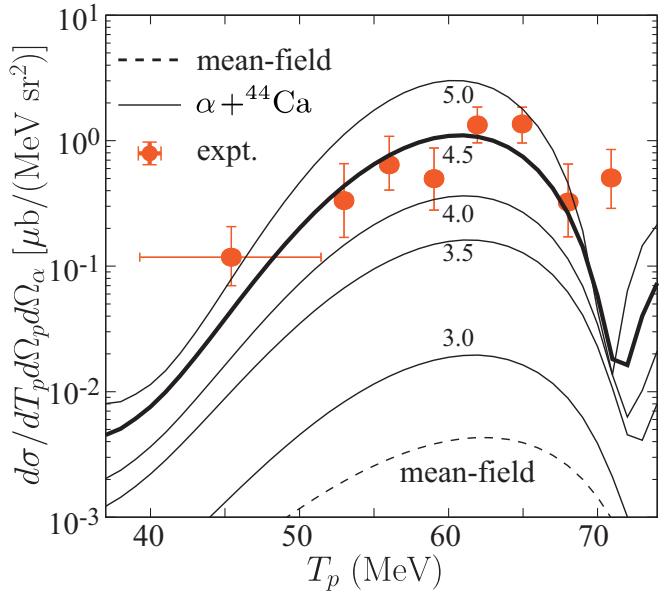

FIG. 3. Triple-differential cross section of ^{48}Ti(p, $p\alpha$)^{44}Ca reaction via DWIA calculations using RWAs of the $\alpha + {}^{44}$Ca (d = 3.0–5.0 fm) and mean-field wave functions shown in Fig. 2(a) and their comparison against experimental results reported by [20]. The incident-proton energy as well as values of the proton and α-particle emission angles equal $E_p = 101.5$ MeV, $\theta_p = -70.0^\circ$, and $\theta_\alpha = 45.0^\circ$, respectively.

probability is much larger than that described by the mean-field solution.

To estimate the degree of α-particle preformation, we used the $\alpha + {}^{44}$Ca wave function to determine RWA values corresponding to different internuclear distances. Figure 3 shows these RWAs to yield cross sections larger than those obtained using the mean-field solution. For every 1-fm increase, this cross section increases by approximately one order of magnitude in terms of the internuclear distance. The RWA values obtained using the $\alpha + {}^{44}$Ca wave function with $d = 4.5$ fm provides the most plausible description of the observed cross section. The peripherality of the (p, $p\alpha$) reaction can be confirmed from the real part of the transition-matrix density (TMD) [28], which can be expressed as

$$\delta(R) = \bar{T}^* \int d\hat{\boldsymbol{R}}\, R^2 F(\boldsymbol{R}) y(R) Y_{00}(\hat{\boldsymbol{R}}). \tag{8}$$

The TMD integral over R equals the square of the transition matrix T. Hence, $\delta(R)$ denotes the distance R at which the reaction occurs. As shown in Fig. 2(b), the TMD value remains negligible in ($R \lesssim 5$ fm) owing to the strong α-particle absorption and small RWA. This explains why the cross section obtained using the mean-field approximation is smaller than that obtained using the $\alpha + {}^{44}$Ca wave function by orders of magnitude. Further, the peak position ($T_p \sim 63$ MeV) and width of the cross section can be determined considering the kinematical condition (recoil-less condition for residue ^{44}Ca) and RWA momentum distribution, respectively. The present microscopic framework has the advantage of evaluating the

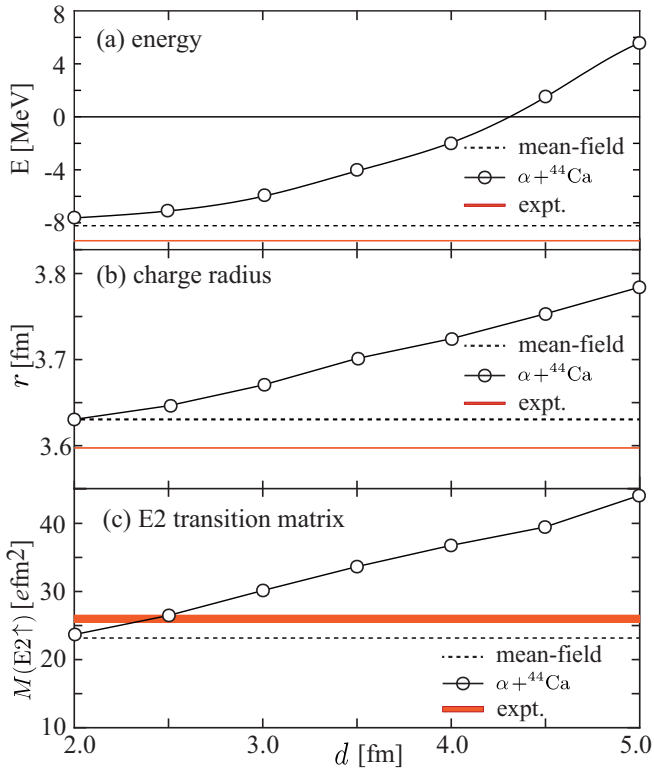

FIG. 4. (a) Binding energy, (b) charge radii, and (c) E2 transition matrix of ^{44}Ti calculated using mean-field solution and $\alpha + ^{44}$Ca wave function, as well as their comparison against experimental data [38–40]. The binding energy is relative to the $\alpha + ^{44}$Ca-decay threshold.

α-particle preformation probability from the knockout cross sections.

Although the $\alpha + ^{44}$Ca wave function corresponding to $d = 4.5$ fm yields the best result for the ^{48}Ti$(p, p\alpha)^{44}$Ca reaction, it must be validated from different perspectives. First, binding energies of the $\alpha + ^{44}$Ca wave function are much smaller than those obtained using the mean-field solution owing to the artificial constraint imposed on the internuclear distance [Eq. (7)]. Figure 4(a) illustrates a rapid decrease in the binding energy of the $\alpha + ^{44}$Ca wave function with an increase in the internuclear distance. At $d = 4.5$ fm, binding-energy value is underestimated by approximately 10 MeV compared to the experimental value [38], and a positive α-decay Q-value is obtained. Contrarily, the mean-field solution yields reasonable binding energy and Q-value. Panels (b) and (c) in Fig. 4 show the charge radius and reduced matrix elements for the E2 transition from the ground to the 2_1^+ states, respectively. As expected, both the charge radius and E2 transition-matrix elements increase with an increase in the internuclear distance. Although the $\alpha + ^{44}$Ca wave function yields reasonable results at $d = 2.0$–2.5 fm, it overestimates those observed at $d = 4.5$ fm [39,40]. Overall, the $\alpha + ^{44}$Ca wave function effectively describes the ^{48}Ti$(p, p\alpha)^{44}$Ca reaction but fails to reproduce the fundamental structural properties. By contrast, the solution obtained using the mean-field approximation better describes the energy, radius, and E2 transition but fails to describe the α-knockout reaction. These results reveal that the ground-state wave function should correspond to a combination of the mean-field solution and $\alpha + ^{44}$Ca-type wave function. Moreover, the mean-field solution should correspond to the dominant ground-state component owing to its large binding energy. However, the $\alpha + ^{44}$Ca wave-function contamination is indispensable from the viewpoint of explaining the observed large α-knockout cross section.

Conclusion. In this study we investigated the ^{48}Ti$(p, p\alpha)^{44}$Ca reaction to explore α-particle preformation in a medium-mass ^{48}Ti nucleus. As observed, the DWIA analysis performed using accurate optical potentials provides a reliable and quantitative description of the α-knockout reaction. The results reveal the α-particle preformation in ^{48}Ti to be unexpectedly enhanced. The mean-field solution is demonstrated to underestimate the differential cross section by at least an order of magnitude. Meanwhile, the $\alpha + ^{44}$Ca wave function, the internuclear distance of which equals $d = 4.5$ fm, accurately estimates this cross section. However, the $\alpha + ^{44}$Ca wave function fails to explain the basic ^{48}Ti properties, which can be reasonably described using the mean-field approximation. Therefore the ground state must correspond to a combination of solutions obtained using the mean-field and $\alpha + ^{44}$Ca configurations. This new insight requires a systematic analysis of the $(p, p\alpha)$ reactions to reveal the universality of the α-particle preformation. This poses a formidable challenge to microscopic nuclear models for describing the α-particle preformation in medium-mass nuclei.

Acknowledgments. This work was supported by the COREnet program of the RCNP, Osaka University, Hattori Hokokai Foundation Grant-in-Aid for Technological and Engineering Research, and JSPS KAKENHI (Grants No. JP16K05352, No. JP18H05407, No. JP18K03617, and No. JP20K14475). Numerical calculations were performed using the Oakforest-PACS at the Center for Computational Sciences, University of Tsukuba, and XC40 at the Yukawa Institute for Theoretical Physics, Kyoto University.

[1] G. Gamow, Zur quantentheorie des atomkernes, Z. Phys. **51**, 204 (1928).
[2] H. J. Mang, Alpha decay, Annu. Rev. Nucl. Sci. **14**, 1 (1964).
[3] D. F. Jackson and M. Rhoades-Brown, Theories of alpha-decay, Ann. Phys. **105**, 151 (1977).
[4] R. G. Lovas, R. J. Liotta, A. Insolia, K. Varga, and D. S. Delion, Microscopic theory of cluster radioactivity, Phys. Rep. **294**, 265 (1998).
[5] C. Qi, R. Liotta, and R. Wyss, Recent developments in radioactive charged-particle emissions and related phenomena, Prog. Part. Nucl. Phys. **105**, 214 (2019).
[6] K. Auranen, D. Seweryniak, M. Albers, A. D. Ayangeakaa, S. Bottoni, M. P. Carpenter, C. J. Chiara, P. Copp, H. M. David, D. T. Doherty, J. Harker, C. R. Hoffman, R. V. F. Janssens, T. L. Khoo, S. A. Kuvin, T. Lauritsen, G. Lotay, A. M. Rogers, J. Sethi, C. Scholey *et al.*, Superallowed

α Decay to Doubly Magic ^{100}Sn, Phys. Rev. Lett. **121**, 182501 (2018).

[7] Y. Xiao, S. Go, R. Grzywacz, R. Orlandi, A. N. Andreyev, M. Asai, M. A. Bentley, G. de Angelis, C. J. Gross, P. Hausladen, K. Hirose, S. Hofmann, H. Ikezoe, D. G. Jenkins, B. Kindler, R. Léguillon, B. Lommel, H. Makii, C. Mazzocchi, K. Nishio *et al.*, Search for α decay of ^{104}Te with a novel recoil-decay scintillation detector, Phys. Rev. C **100**, 034315 (2019).

[8] R. M. Clark, A. O. Macchiavelli, H. L. Crawford, P. Fallon, D. Rudolph, A. Såmark-Roth, C. M. Campbell, M. Cromaz, C. Morse, and C. Santamaria, Enhancement of α-particle formation near ^{100}Sn, Phys. Rev. C **101**, 034313 (2020).

[9] F. Mercier, J. Zhao, R. D. Lasseri, J. P. Ebran, E. Khan, T. Nikšić, and D. Vretenar, Microscopic description of the self-conjugate ^{108}Xe and ^{104}Te α -decay chain, Phys. Rev. C **102**, 011301(R) (2020).

[10] S. Yang, C. Xu, G. Röpke, P. Schuck, Z. Ren, Y. Funaki, H. Horiuchi, A. Tohsaki, T. Yamada, and B. Zhou, α decay to a doubly magic core in the quartetting wave function approach, Phys. Rev. C **101**, 024316 (2020).

[11] J. Tanaka, Z. Yang, S. Typel, S. Adachi, S. Bai, P. van Beek, D. Beaumel, Y. Fujikawa, J. Han, S. Heil, S. Huang, A. Inoue, Y. Jiang, M. Knösel, N. Kobayashi, Y. Kubota, W. Liu, J. Lou, Y. Maeda, Y. Matsuda *et al.*, Formation of α clusters in dilute neutron-rich matter, Science **371**, 260 (2021).

[12] K. Ikeda, N. Takigawa, and H. Horiuchi, The systematic structure-change into the molecule-like structures in the self-conjugate 4N nuclei, Prog. Theor. Phys. Suppl. **E68**, 464 (1968).

[13] K. Wildermuth and Y. C. Tang, *A Unified Theory of the Nucleus* (Vieweg+Teubner Verlag, Wiesbaden, 1977).

[14] E. G. Adelberger, S. M. Austin, J. N. Bahcall, A. B. Balantekin, G. Bogaert, L. S. Brown, L. Buchmann, F. E. Cecil, A. E. Champagne, L. De Braeckeleer, C. A. Duba, S. R. Elliott, S. J. Freedman, M. Gai, G. Goldring, C. R. Gould, A. Gruzinov, W. C. Haxton, K. M. Heeger, E. Henley *et al.*, Solar fusion cross sections, Rev. Mod. Phys. **70**, 1265 (1998).

[15] P. Descouvemont and D. Baye, The R-matrix theory, Rep. Prog. Phys. **73**, 036301 (2010).

[16] Y. Fujiwara, H. Horiuchi, K. Ikeda, M. Kamimura, K. Kato, Y. Suzuki, and E. Uegaki, Chapter II. Comprehensive study of alpha-nuclei, Prog. Theor. Phys. Suppl. **68**, 29 (1980).

[17] R. Bijker and F. Iachello, Cluster structure of light nuclei, Prog. Part. Nucl. Phys. **110**, 103735 (2020).

[18] P. G. Roos, N. S. Chant, A. A. Cowley, D. A. Goldberg, H. D. Holmgren, and R. Woody, Absolute spectroscopic factors from the (p, pα) reaction at 100 MeV on 1p-shell nuclei, Phys. Rev. C **15**, 69 (1977).

[19] A. Nadasen, N. S. Chant, P. G. Roos, T. A. Carey, R. Cowen, C. Samanta, and J. Wesick, Non-coplanar (p, $p\alpha$) and (p, d ^{3}He) reactions on ^{9}Be at 101.5 MeV, Phys. Rev. C **22**, 1394 (1980).

[20] T. A. Carey, P. G. Roos, N. S. Chant, A. Nadasen, and H. L. Chen, Alpha-particle spectroscopic strengths using the (p, p) reaction at 101.5 MeV, Phys. Rev. C **29**, 1273 (1984).

[21] T. Yoshimura, A. Okihana, R. E. Warner, N. S. Chant, P. G. Roos, C. Samanta, S. Kakigi, N. Koori, M. Fujiwara, N. Matsuoka, K. Tamura, E. Kubo, and K. Ushiro, Alpha spectroscopic factors for ^{6}Li, ^{7}Li, ^{9}Be and ^{12}C from the (p, $p\alpha$) reaction at 296 MeV, Nucl. Phys. A **641**, 3 (1998).

[22] J. Mabiala, A. A. Cowley, S. V. Förtsch, E. Z. Buthelezi, R. Neveling, F. D. Smit, G. F. Steyn, and J. J. Van Zyl, Analyzing power and cross section distributions of the ^{12}C(p, $p\alpha$)^{8}Be cluster knockout reaction at an incident energy of 100 MeV, Phys. Rev. C **79**, 054612 (2009).

[23] K. Yoshida, Y. Chiba, M. Kimura, Y. Taniguchi, Y. Kanada-En'yo, and K. Ogata, Quantitative description of the ^{20}Ne (p, $p\alpha$) ^{16}O reaction as a means of probing the surface α amplitude, Phys. Rev. C **100**, 044601 (2019).

[24] T. Delbar, G. Grégoire, G. Paic, R. Ceuleneer, F. Michel, R. Vanderpoorten, A. Budzanowski, H. Dabrowski, L. Freindl, K. Grotowski, S. Micek, R. Planeta, A. Strzalkowski, and K. A. Eberhard, Elastic and inelastic scattering of alpha particles from ^{40,44}Ca over a broad range of energies and angles, Phys. Rev. C **18**, 1237 (1978).

[25] S. Hama, B. C. Clark, E. D. Cooper, H. S. Sherif, and R. L. Mercer, Global Dirac optical potentials for elastic proton scattering from heavy nuclei, Phys. Rev. C **41**, 2737 (1990).

[26] E. D. Cooper, S. Hama, B. C. Clark, and R. L. Mercer, Global Dirac phenomenology for proton-nucleus elastic scattering, Phys. Rev. C **47**, 297 (1993).

[27] K. Yoshida, K. Minomo, and K. Ogata, Investigating α clustering on the surface of ^{120}Sn via the (p, $p\alpha$) reaction, and the validity of the factorization approximation, Phys. Rev. C **94**, 044604 (2016).

[28] T. Wakasa, K. Ogata, and T. Noro, Proton-induced knockout reactions with polarized and unpolarized beams, Prog. Part. Nucl. Phys. **96**, 32 (2017).

[29] K. Yoshida, K. Ogata, and Y. Kanada-En'yo, Investigation of α clustering with knockout reactions, Phys. Rev. C **98**, 024614 (2018).

[30] E. D. Cooper, S. Hama, and B. C. Clark, Global Dirac optical potential from helium to lead, Phys. Rev. C **80**, 034605 (2009).

[31] Y. Kanada-En'yo, M. Kimura, and H. Horiuchi, Antisymmetrized molecular dynamics: A new insight into the structure of nuclei, C. R. Phys. **4**, 497 (2003).

[32] Y. Kanada-En'yo, M. Kimura, and A. Ono, Antisymmetrized molecular dynamics and its applications to cluster phenomena, Prog. Theor. Exp. Phys. **2012**, 1A202 (2012).

[33] M. Kimura, T. Suhara, and Y. Kanada-En'yo, Antisymmetrized molecular dynamics studies for exotic clustering phenomena in neutron-rich nuclei, Eur. Phys. J. A **52**, 373 (2016).

[34] J. Berger, M. Girod, and D. Gogny, Time-dependent quantum collective dynamics applied to nuclear fission, Comput. Phys. Commun. **63**, 365 (1991).

[35] Y. Chiba and M. Kimura, Laplace expansion method for the calculation of the reduced-width amplitudes, Prog. Theor. Exp. Phys. **2017**, 053D01 (2017).

[36] Y. Taniguchi, M. Kimura, and H. Horiuchi, New constraint of clustering for AMD and its application to the study of the $2\alpha-^{12}$C structure of ^{20}Ne, Prog. Theor. Phys. **112**, 475 (2004).

[37] Y. Taniguchi and M. Kimura, ^{12}C+^{16}O molecular resonances at deep sub-barrier energy, Phys. Lett. B **800**, 135086 (2020).

[38] W. J. Huang, G. Audi, M. Wang, F. G. Kondev, S. Naimi, and X. Xu, The AME2016 atomic mass evaluation (I). Evaluation of input data; And adjustment procedures, Chin. Phys. C **41**, 030002 (2017).

[39] I. Angeli and K. P. Marinova, Table of experimental nuclear ground state charge radii: An update, At. Data Nucl. Data Tables **99**, 69 (2013).

[40] T. W. Burrows, Nuclear data sheets for A = 48, Nucl. Data Sheets **107**, 1747 (2006).